Available online at www.sciencedirect.com

ScienceDirect

Procedia CIRP 133 (2025) 346–351

www.elsevier.com/locate/procedia

20th CIRP Conference on Modeling of Machining Operations

Improved coolant channel flow efficiency for grooving tools through simulation and additive manufacturing

Patrick Fischmann, Sebastian Galland, Frederik Zanger*

wbk Institute of Production Science, Karlsruhe Institute of Technology (KIT), Kaiserstraße 12, 76131 Karlsruhe, Germany

* Corresponding author. E-mail address: frederik.zanger@kit.edu

Abstract

Laser-based powder bed fusion for metals (PBF-LB/M) enables the production of complex external and internal shapes. This enables tool production with targeted supply of cooling lubricant. The simulative channel design and the resulting increase in coolant flow after production are the focus of this work. The optimization process is illustrated using a commercially available grooving tool with three channels and four outlets. Accordingly, a simulation was conducted to investigate and ultimately reduce the pressure loss between the inlet and outlet of the channel. This approach resulted in a calculated reduction in pressure loss of up to 97 % in the channels, as well as increased uniformity of the stream at the coolant outlet. After production of the optimized tool using PBF-LB/M, a volume flow measurement was conducted under varying coolant pressure. Fluctuations between the different tool holders were observed, which can be attributed to the additive manufacturing process and resulting spatter. In relation to all cooling channels in the grooving tool, an increase in the flow rate of up to 6% was determined.

Keywords: Additive Manufacturing; Computational Fluid Dynamics; Roughness

1. Introduction

Additive manufacturing offers significant advantages for machining, which are particularly beneficial in the production of tool bodies with conventionally manufactured cutting edges. The flexibility of additive manufacturing enables the design of complex internal channels for directed coolant supply and allows for advanced topology optimization, among other applications.

The targeted supply of cooling lubricant can significantly reduce thermomechanical wear mechanisms during machining by improving the cooling and lubricating effect in the contact zone. In [1] for example, a 12% reduction in wear during grooving with an additively manufactured (PBF-LB/M) tool holder is shown when coolant was additionally supplied to the side cutting edges of the indexable insert. Another study [2] showed a reduction in the contact area between the rake face and chip, a lower chip volume due to tighter curling, and reduced tool wear on the flank face when using PBF-LB/M manufactured milling cutter heads with targeted coolant supply. Furthermore, optimized shapes and sizes of additively manufactured internal coolant channels can be used to increase the jet velocity [3]. A detailed simulation-based approach for a cutter head can be found in [4]. The nozzle design can help to shape and focus the free jet depending on the application. However, powder adhesion and surface roughness in powder bed-based laser beam melting (PBF-LB/M) prevent an accurate prediction of the free jet geometry. In [5], it is shown that additively manufactured milling cutters have a longer tool life and reduced wear rates compared to conventionally manufactured ones. This results from the already described manufacturing option in PBF-LB/M of being able to insert optimized cooling channels with directed media supply. The work identified a need for further research to analyze the

2212-8271
10.1016/j.procir.2025.02.060

vibration behavior of additively manufactured milling tools in detail. Various materials are to be investigated with regard to their wear behavior in order to evaluate the effectiveness of L-shaped coolant nozzles. In addition, the authors emphasized the need for post-processing of the cooling channels to achieve a smoother surface and improved coolant supply. Another work demonstrates optimized internal channel designs for improved coolant flow [6]. By changing from a sharp-edged channel to one with a radius, the volume flow could be increased by approx. 23 %. However, it was not possible to achieve the defined tolerances of the additive manufacturing of the indexable insert milling cutter, so that post-processing by machining is necessary. In [7], a process optimization through adapted particle size distribution is shown, which reduces roughness at large overhangs. In the case of topology optimizations, which, in addition to the classic weight saving, also include a simulative approach to cooling channel design, it can be seen that a compromise between rigidity and optimization target must be made in order to achieve a high level of efficiency for the optimized tool on the one hand and its structural integrity on the other [8].

The focus of the paper is to demonstrate the potential of simulative channel design to increase the flow rates that are to be demonstrated in the experiment. In addition, the influence of the roughness generated in the process is evaluated, which is varied by means of adapted particle size distributions. Both approaches are intended to demonstrate the optimization potential of additive manufacturing.

2. Materials and methods

2.1. Grooving tool

The investigations were carried out based on the same grooving tool with three cooling channels as in [1]. In Fig. 1, the designation of the individual channels is inserted. The channel RF feeds the medium to the rake face, the channel FF to the flank face, and the SCE channel splits inside the tool and feeds the two secondary cutting edges. The tool is manufactured from tool steel 1.2709 using PBF-LB/M.

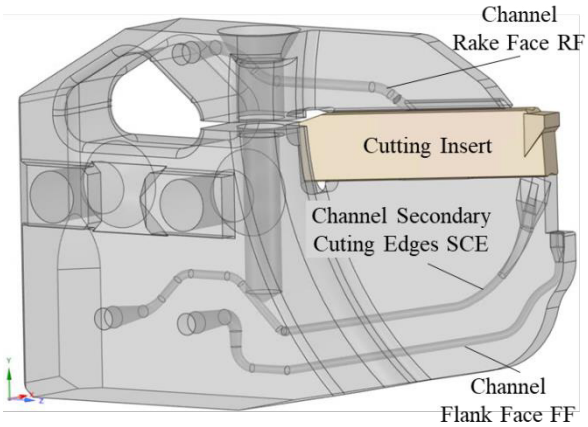

Fig. 1. The investigated cutting tool with the three channels RF, FF and SCE

2.2. Channel optimization

The tool optimization was carried out incrementally, the approach is roughly described in this paragraph and explained in detail afterwards. Initially, a simulation study was carried out for the FF channel and the methodology was applied to the RF and SCE channels. The computational fluid dynamics (CFD) software Ansys Fluent (version 2023 R1), was employed to optimize the cooling channels towards minimizing the pressure drop between the inlet and outlet of all three channels. The original geometry of the channels was deemed to be too far away from an optimal design. A geometry-related low mesh quality due to sharp edges and flow instabilities caused by the geometry, see the pathlines in Fig. 2 a) and c), resulted in unstable calculations and optimizations. Hence, a substitute geometry was designed for all three channels, see Fig 2 b) and d). This substitution geometry eliminated sharp corners, access material and connected the inlet and outlet directly. A mesh was generated, using Ansys own meshing tool, and subsequently verified in a mesh convergence study to ensure accuracy. This mesh was then used as basis for the calculations in Fluent. To optimize the geometry towards pressure-drop the Adjoint Solver was used. The Adjoint Solver is a tool build into Ansys Fluent, which uses an iterative approach to optimize geometries towards many selectable variables, called observables. In a first step the fluent calculation (CFD) is performed until convergence is reached. After this, the Adjoint calculations are conducted. In this step sensitivities (Fig. 3) are identified to optimize for the selected observable. Once this is done, the geometry is morphed and the process starts again. This is repeated until the set convergence criterion for change in the observable is met.

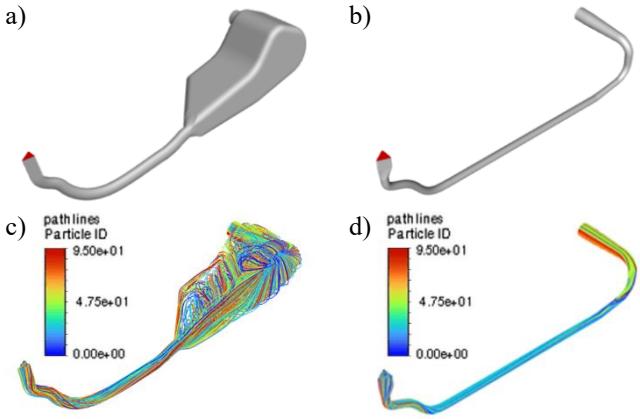

Fig. 2. Channel Flank Face a) original geometry, b) substitution geometry, c) pathlines original geometry, d) pathlines substitution geometry.

Due to Ansys Fluent´s reliance on the finite element method a mesh had to be created. For the creation of the mesh the meshing tool built into Ansys Fluent was used. A surface mesh was generated using a minimum cell size of 0.0001 mm, a maximum cell size of 0.1 mm and the growth rate was set to 1.1. For the size functions Ansys offers curvature, proximity and curvature & proximity. The curvature setting was chosen, as due to a lack of surfaces in direct proximity to each other choosing curvature & proximity was deemed unnecessary. The

curvature normal angle was set to nine degrees. Ten boundary layers were added using the offset method type last ratio with

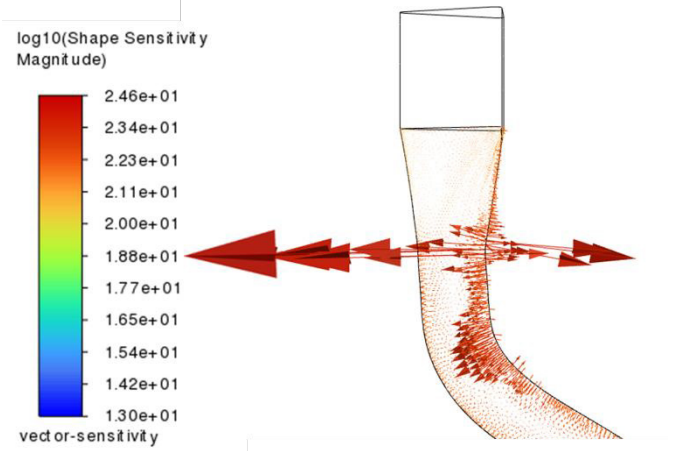

Fig. 3. Sensitivities for the Adjoint Optimization near the outlet of channel FF

a transition ratio of 0.333 and a first height of 0.001 mm. Finally, the volume mesh was generated using polyhedral cells due to their superior morphing capabilities compared to tetrahedral meshes [9]. The growth rate was set to 1.1 and the maximum cell length was set to 0.1, copying the settings for the surface mesh. Those settings led to a mesh consisting of 695 167 cells, 2 078 474 nodes and 3 239 121 faces. The before mentioned settings for the cell size for both the surface and volume mesh were chosen through a mesh convergence study. This was done by creating a coarse mesh with large maximum and minimum cell sizes and then incrementally reducing those values step by step, keeping the maximum cell size 1 000 times the minimum cell size. Those meshes were then evaluated in Fluent and the outlet velocities were compared. When the change in velocity between a mesh and its predecessor was lower than 1 % the convergence criterion was met, and the mesh was chosen for calculation. The resulting settings were then applied to channel SCE and RF.

The calculations were conducted using the double precision setting, allocating 64 bits instead of 32 bits for every floating-point number, reducing rounding errors. Water was used as the medium flowing through the channels at a velocity of 50 m/s.

It was determined that the rough elements, resulting from the PBF-LB process, protrude into the fully turbulent region of flow, thereby destroying the viscous sublayer [10]. To simulate this, the sand-grain roughness of the walls was set to 40 µm. This value was chosen due to the roughness values shown in [7]. At a low build angle, surface roughness is up to $S_a = 62$ µm, whereas sideskin roughness has a lower value of about $S_a = 10$ µm. Since build angles $< 45°$ dominate in the channels SCE and FF, the value was set higher than the mean value. As the turbulence model the SST K-Omega model was chosen, which is a combined model for predicting free flow and the flow near surfaces [11]. Before utilizing the Adjoint Solver, it was ensured that the flow calculations would fully converge. Subsequently the pressure drop between the inlets and outlets of the channels was specified as the observable for the Adjoint Solver with a target reduction of 15 % per iteration of the Adjoint Solver and a convergence criterion of 1e-5 was set up. The solution methods for the Flow Solver and Adjoint Solver were set up to be consistent. Specifically, the following settings were applied: for the gradient scheme, the least squares cell-Based method; for pressure discretization, the second-order scheme; and for momentum discretization, the second-order upwind scheme. For the stabilization strategy a blended type was applied, with 10 iterations in the first scheme and 40 iterations in the second scheme was set to residual minimization. To ensure a minimal wall thickness and prevent any interference of the individual channels a design-condition was added. In this so called bound by surfaces condition, an outer perimeter for the mesh morphing calculated by the Adjoint Solver, is created via surfaces surrounding the channel, see Fig. 4.

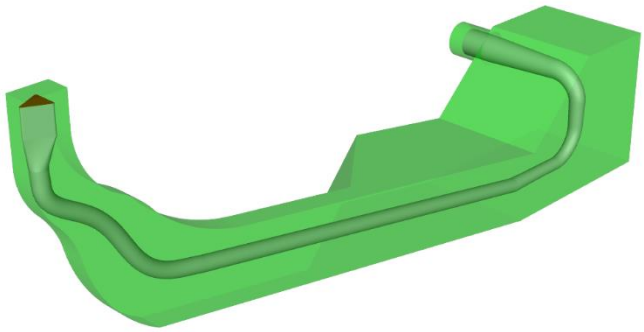

Fig. 4. Design-Condition to prevent break throughs

The Adjoint Solver offers three different morphing methods: polynomials, radial basis function and direct interpolation. The direct interpolation morphing method has only one sub setting called smoothness. Values of 0.05, 0.5 and 5 were tested. Radial basis function offers the additional setting of a constraint method with the choice between standard and enhanced. Polynomials offer the widest range of sub settings with a choice between the standard or enhanced constrain methods and a so-called freeform scaling scheme with the choice between control-point spacing and objective reference change, that only exists within the standard constraint method. Tests with all these mentioned sub settings were conducted and the results were compared to choose the best approach for the Adjoint Optimization.

2.3. Production

The production of the cutting tool was performed based on findings from previous work, where the influence of particle size distribution on surface roughness in powder bed fusion [7] was researched. Based on these findings, two different powders were chosen. First, the commercially available powder was used. The tools manufactured with this powder are named CAP. Second, the powder with the increased fine content with lower roughness was used. Following the naming, the tool manufactured using this powder are called FP. These two tools are used to compare the influence of the manufacturing process on the flow rate. Seven tools were produced from each powder type to enable a statistical analysis to be carried out. Detailed information on the machine, powder and process control variables can be found in [7]. After the additive manufacturing, a heat treatment and the necessary machining was performed. Both tool types are compared with currently available grooving tools, these serve as a reference base, called RB.

2.4. Volume flow

The printed grooving tools were used to conduct tests of the volume flow. The measurements of the flowrate were taken with a DUM/A-28 flow monitor (Meister Strömungstechnik GmbH, Wiesen). The analysis of the flow rates was performed on a DMG DMU 60 eVo FD milling machine, outfitted with a frequency-controlled high-pressure pump. With this pump coolant pressures of 8-80 bar can be achieved. During the tests the pressure was varied in 5 steps: 8, 20, 40, 60 and 80 bar. The coolant used was SWISSCOOL 8000 made by Motorex (Langenthal, Switzerland), in a water-based emulsion of 7 %. For each step the flowrates were recorded, first for the individual channels and then for the combined channels.

2.5. Computer tomography

After the flow test, the cutting tools with remarkable flow rates were measured in a computer tomograph (CT). The device used is a Metrotom 1500 (Carl Zeiss Industrielle Messtechnik GmbH, Oberkochen). Due to the pronounced asymmetry, parameter determination was complex. The different X-ray penetration thicknesses (minimum 2.5 mm, maximum 44 mm) did not allow an overall image of the tool in sufficient quality to be taken. For this reason, only the actual cutting blade was measured, whereby the maximum X-ray penetration length was reduced and results could be generated. The selected parameters are a voltage of 225 kV, a current of 180 µA at an integration time of 1 000 ms and a gain of six. To reduce artefacts, a copper filter with a thickness of 0.5 mm was used, and the reconstruction was carried out with the Feldkamp algorithm. Even with the optimised settings, the geometry shows artefacts, but these are not in the region of interest. The results were evaluated using the software VG Studio Max (Volume Graphics GmbH, Heidelberg).

3. Results

3.1. Channel optimization

In the early stages of testing, it was observed that the Adjoint Solver had the tendency to distort the inlets and outlets of the channels, even though these were excluded in the zones set for modification by the program. To combat this tendency buffer zones were created on both the inlet and the outlet, which were not included in the parts of the channels to be modified by the Adjoint Solver. Additionally, the region in which the design-tool was allowed to make changes was set up to exclude both openings of the channels. This approach succeeded in forcing the Adjoint Solver to only morph the geometry in the designated areas. In search of the optimal morphing method for reducing the pressure drop in combination with a bounded by surface constraint tests with all three morphing methods, and their respective sub setting, offered by the design tool of the Adjoint Solver, were conducted.

For the direct interpolation method, varying the smoothness setting between 0.05, 0.5 and 5 provided relatively consistent results. A smoothness value of 0.05 achieved a 93.64 % reduction in pressure drop over 163 iterations, while a value of 0.5 resulted in a 95.49 % reduction in 71 iterations. Similarly, a smoothness value of 5 produced a 94.63 % reduction in just 55 iterations. In all cases, the pressure drop reduction was accomplished by evenly widening the channel along its entire length as it can be seen in Fig. 5 b). The results for the radial basis function morphing method were calculated with the two constraint methods standard and enhanced. The standard calculation converged after just 2 design iterations. This rapid convergence occurred because the Adjoint Solver predicted an increase in pressure drop. This result was verified by repeating the calculation. The pressure drop did therefore only decrease by 0,66 %. In contrast the enhanced constraint method converged after 96 iterations with very little change in geometry and a pressure loss reduction of 18,47 %. The two polynomials calculations using the constraint method standard and the freeform scaling scheme of either control point spacing or object reference change yielded in identical results. 14 iterations with moderate geometry change were calculated until the convergence criterion was met and the pressure drop was decreased by 84,94 %. As Fig. 5. c) shows this reduction was achieved by widening the channel near the outlet and creating a cavity in the first bend right behind the inlet. Lastly, the combination of the polynomials morphing method and the enhanced constraint method was tested. The Adjoint Solver calculated 48 iterations and produced a reduction in pressure drop of 97,33 %. This combination of settings produced the highest amount of geometry deformation and thereby also achieved the biggest reduction in pressure drop out of all tested setting combinations. But as it is visible in Fig. 5. d), the mesh is warped drastically in multiple places hindering flow and making production difficult. In addition to the reduction in pressure drop, the changes in the geometry also led to a homogenisation of the outlet velocity.

This effect is most pronounced in the calculations that demonstrated the greatest reduction in pressure drop and the most significant degree of mesh morphing. For selecting the

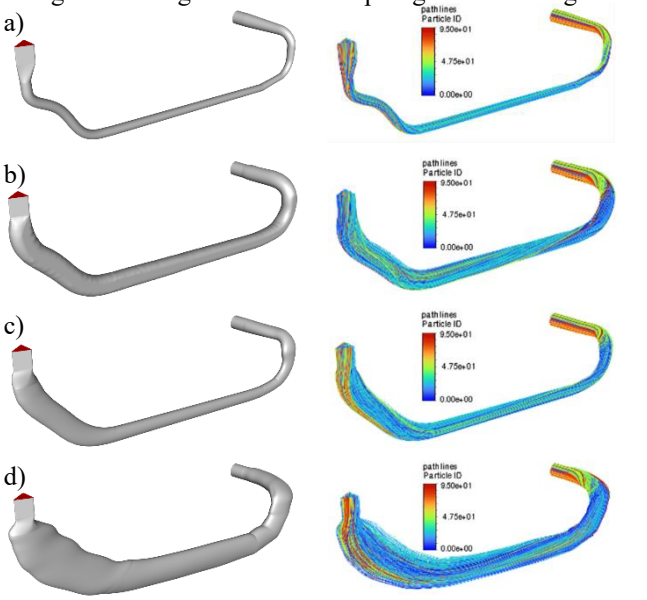

Fig. 5. Results of the Adjoint Optimization. On the left geometry, on the right pathlines. a) Substitution geometry. b) Direct Interpolation; Smoothness 0.5. c) Polynomials; constraint method Standard. d) Polynomials; constraint method Enhanced.

simulation to produce the grooving tool, the combination of the polynomials morphing method and enhanced constraint method was initially considered. However, concerns about mechanical instability due to excessive warping led to the adoption of the direct interpolation morphing method with a smoothness parameter of 0.5. Although the polynomials approach achieved a slightly higher pressure drop reduction (97.33% compared to 95.49%), the direct interpolation method was favoured due to its smoother geometry and nearly identical outlet velocity homogenization, see Fig. 6, making it a more reliable and practical choice.

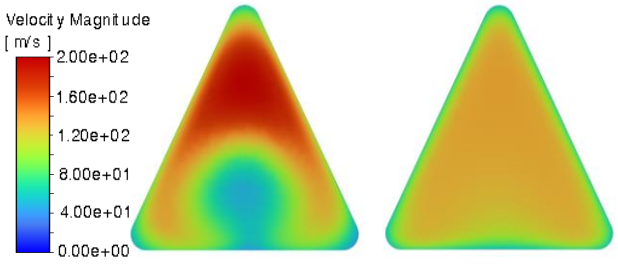

Fig. 6. Outlet velocity at the exit of channel FF. Substitution geometry left, result Direct Interpolation with 0.5 smoothness right.

3.2. Volume flow

As illustrated in Fig. 7 the three different tool types demonstrated comparable performances across the different pressure levels. At a pressure of 8 bar, the flow rate across all channels is approximately 4.4 l/min. Increasing the pressure to 20 bar results in a flow rate of around 7 litres per minute, representing a 56 % increase. Further raising the pressure to 40 bar increases the flow rate to approximately 10.5 l/min, a 51 % increase. Increasing the pressure even further to 60 bar leads to a flow rate of about 12.5 l/min, an increase of around 20 %. The final pressure increase to 80 bar yields a flow rate of 14.3 l/min, resulting in only a 13 % improvement. The further the pressure is increased, the more the percentual increases in flow rate is diminished. It is noticeable, that the grooving tool fabricated from the commercially available powder (CAP) has the lowest standard deviation between the tested grooving tools with only one minor outlier towards the top, while both the RB and the FP tools have multiple tools that are downward outliers.

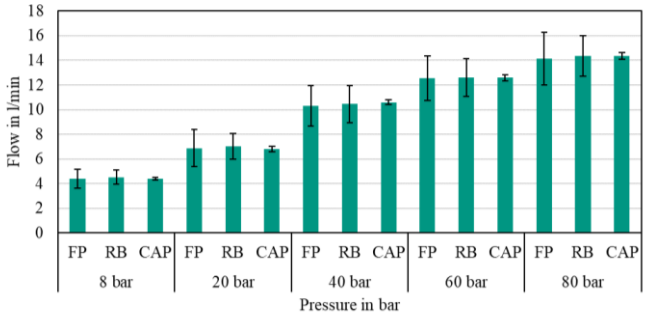

Fig. 7. Flow rates of the manufactured tools at varying pressure.

In Fig. 8, a closer look inside the flow rate of the channel SCE of the tools FP at 80 bar pressure is taken. Four of the seven tools show minimal deviation in the flow rate. With the other three tools, the flow rate drops significantly, in some cases by up to 62 %. While the SCE channel is inconstant as described, the RF and FF channels show reduced deviations, with the measurements showing no classic outliers. The values for RF fluctuate between 4.55 and 3.83 l/min, and for FF between 4.57 and 4.78 l/min. The observations for the last two channels can be transferred to the channels of the other grooving tools. Solely in one RB-type tool the flow is reduced in the channel SCE.

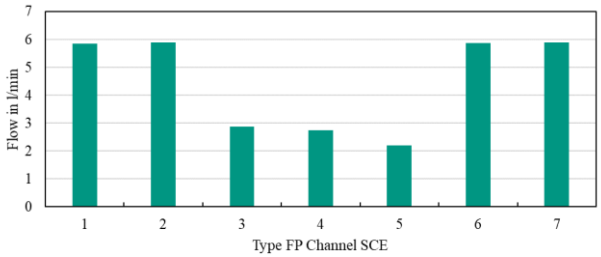

Fig. 8. Flow rates in the channel SCE of the seven manufactured tools, using FP powder.

In order to gain a deeper insight into the potential of the optimized grooving tools and the process optimization from [7], the outliers have been removed from the measurement data in Fig. 9. Consequently, the FP type shows the highest flow rate, followed by the RB and CAP types. The standard deviation is still highest for the FP type.

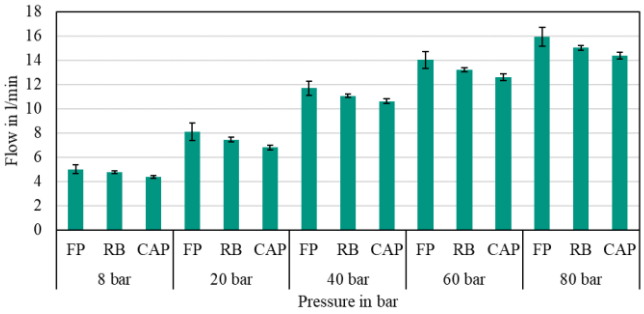

Fig. 9. Flow rates of the manufactured tools at varying pressure after removal of outliers

4. Discussion

The Adjoint Solver produces intriguing results, although these vary considerably depending on the settings selected. Furthermore, the final outcome is influenced by the initial geometry, which can lead to stability issues and, consequently, simulation crashes during optimisation. Due to the intricate nature of the geometry, a selection based on numbers or data is not feasible. However, the engineer must also consider the manufacturability of the tool.

Furthermore, an exact selection of the settings is complex. In our application, the additive manufacturing of the grooving tools in PBF-LB/M, the settings for the roughness are even more complex. As shown in [7], the surface roughness in additive manufacturing varies depending on the particle size distribution and the surface orientation. Ansys Fluent or the Adjoint Solver does not allow for detailed settings of the roughness in the GUI – in this work, the sand grain roughness was used. This is a strong simplification of the real process-related roughness and thus forms a deviation between the simulation result and the experiment. This is also why the CAP type shows a poorer performance than the FP and even RB type

in the adjusted flow rates. A sand grain roughness of 40 µm was assumed in the optimization. The actual roughness between the CAP and FP types differs, which is why the simulation is probably closer to the FP type than to the CAP type, and thus the flow properties are insufficiently modelled.

Furthermore, a more in-depth analysis of the fluctuations in the flow rate must be carried out. Although the FP type shows the best results when adjusted, the production cannot be considered stable due to the strong fluctuations. This is more pronounced in the FP type, but it is also evident in the other types. Fig 10 shows the cross section in the cutting tool, focusing on the channel FF and SCE. Due to the artefacts during reconstruction, a qualitative examination is carried out below. The roughness on the up- and downskin as well as unwanted material accumulations in the channel can be seen in the images. The up- and downskin are unavoidable due to the geometry and manufacturing process, the build direction (BD) leads to the surface orientations. Qualitatively, it can be seen that the roughness on the upper side in the FF channel is lower for type FP (Fig. 10. a) & b)) than for types CAP and RB (Fig. 10. c) & d)). This confirms the findings from [7] and the transfer to complex geometries. In b) and d), however, material accumulations can also be clearly seen in the SCE channel, which reduces the flow rate. These result from process instabilities in PBF-LB, which are shown, for example, in [12]. Spatter, which can be many times larger than the powder, can weld in unwanted places and thus lead to defects. With a channel diameter of approx. 1.5 mm, even slight welding can have a negative effect. It is assumed that the FP powder leads to increased spatter formation and thus the process fluctuations are more pronounced.

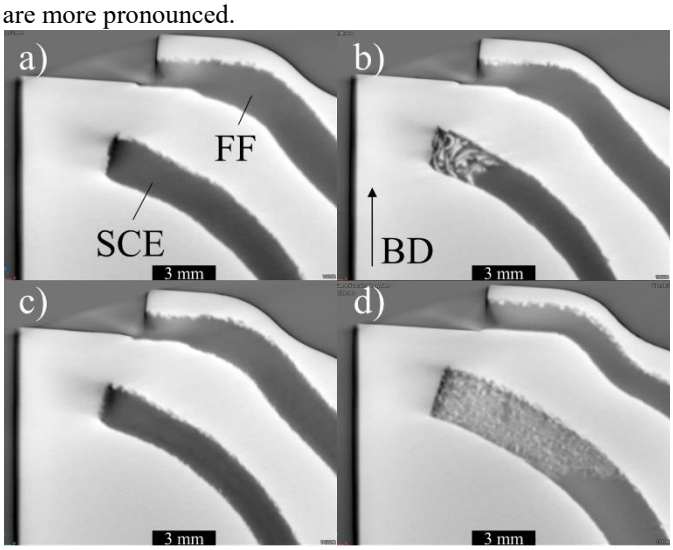

Fig. 10. CT images, cross-section view. a) FP no. 1, high flow, b) FP no. 5, low flow, c) CAP no. 5, d) RB no. 1

5. Conclusion

This study demonstrates the potential of additive manufacturing (AM), specifically powder bed fusion with laser beam melting (PBF-LB/M), for optimizing grooving tools through simulative channel design and tailored particle size distributions. The optimized geometries achieved notable reductions in pressure drop and enhanced flow rate performance, demonstrating the advantages of the Adjoint Solver in computational fluid dynamics (CFD) optimization. Among the morphing methods tested, the direct interpolation method with a smoothness value of 0.5 emerged as a reliable balance between manufacturability, pressure reduction, and flow homogenization.

However, significant challenges remain. The impact of AM-related surface roughness, modelled as sand-grain roughness in the simulation, introduces deviations between simulated and experimental results. The discrepancies highlight the limitations of current simulation tools in accurately representing process-related roughness. Additionally, the production variability, particularly in the FP tools, indicates the need for process stabilization or appropriate post-processing to achieve consistent tool quality.

Acknowledgements

The authors thank the Ministry of Science, Research and Arts of the Federal State of Baden-Württemberg and the Rosswag GmbH for the financial support of the project within the Innovation Campus Future Mobility (ICM).

References

[1] Lubkowitz, V.; Reothia, N.; Zanger, F.: Enhancement of groove turning performance by additively manufactured tool holders with internal cooling channels and combined cooling strategies, in Proceedings of the Machining Innovations Conference for Aerospace Industry (MIC), 2021.

[2] Kelliger, T.; Meurer, M.; Bergs, T.: Efficient Cutting Fluid Supply in Additively Manufactured Indexable Helical Milling Tools for Roughing of Ti-6Al-4V, in Proceedings of the Machining Innovations Conference for Aerospace Industry (MIC), 2023.

[3] Sykora, J.; Kroft, L.: Additive Manufacturing of Indexable Inserts: New Possibilities for more Effective Cooling, in Proceedings of the 32nd DAAAM International Symposium, 2021. DOI: 10.2507/32nd.daaam.proceedings.057.

[4] Kelliger, T.; Liu, H.; Schraknepper, D.; Bergs, T.: Investigations on the Impact of Additively Manufactured Coolant Channels and Outlet Nozzles on Free Jet and Jet Forces in High-Pressure Cutting Fluid Supply, in Proceedings of the Machining Innovations Conference for Aerospace Industry (MIC), 2021.

[5] Lakner, T.; Bergs, T.; Döbbeler, B.: Additively manufactured milling tool with focused cutting fluid supply. Procedia CIRP 81, S. 464–469, 2019. DOI: 10.1016/j.procir.2019.03.118.

[6] Zachert, C.; Liu, H.; Lakner, T.; Schraknepper, D.; Bergs, T.: CFD simulation to optimize the internal coolant channels of an additively manufactured milling tool. Procedia CIRP 102, S. 234–239, 2021. DOI: 10.1016/j.procir.2021.09.040.

[7] Fischmann, P., Schrauth, F., & Zanger, F. (2023). Influence of particle size distribution on surface roughness in powder bed fusion-A contribution to increase resource efficiency. *CIRP Annals*, *72*(1), 145-148.

[8] Kennametal Revs Up Metal Cutting Innovation with 3D Printed Tool for Automotive Supplier Voith. https://www.kennametal.com/us/en/about-us/news/kennametal-revs-up-metal-cutting-innovation-with-3d-printed-tool.html, 2024.

[9] Gain, A. L., Paulino, G. H., Duarte, L. S., & Menezes, I. F. (2015). Topology optimization using polytopes. *Computer Methods in Applied Mechanics and Engineering*, *293*, 411-430.

[10] Kadivar, M., Tormey, D., & McGranaghan, G. (2021). A review on turbulent flow over rough surfaces: Fundamentals and theories. *International Journal of Thermofluids*, *10*, 100077.

[11] Menter, F. R. (1994). Two-equation eddy-viscosity turbulence models for engineering applications. AIAA journal, 32(8), 1598-1605.

[12] Berez, J., & Saldaña, C. (2024). On the nature and causes of spatter redistribution in laser powder bed fusion. *Journal of Manufacturing Processes*, *127*, 531-544.